Appl. Sci. Converg. Technol. 26(6): 201-207 (2017)
http://dx.doi.org/10.5757/ASCT.2017.26.6.201

Research Paper

Electron-excitation Temperature with the Relative Optical-spectrumIntensity in an Atmospheric-pressure Ar-plasma Jet

Gookhee Han and Guangsup Cho*
Department of Electrical and Biological Physics, Kwangwoon University, Seoul 139-701, Korea

Received October 30, 2017; revised November 14, 2017; accepted November 22, 2017

Abstract An electron-excited temperature (T_{ex}) is not determined by the Boltzmann plots only with the spectral data of 4p→4s in an Ar-plasma jet operated with a low frequency of several tens of kHz and the low voltage of a few kV, while T_{ex} can be obtained at least with the presence of a high energy-level transition (5p→4s) in the high-voltage operation of 8 kV. The optical intensities of most spectra that are measured according to the voltage and the measuring position of the plasma column increase or decay exponentially at the same rate as that of the intensity variation; therefore, the excitation temperature is estimated by comparing the relative optical-intensity to that of a high voltage. In the low-voltage range of an Ar-jet operation, the electron-excitation temperature is estimated as being from 0.61 eV to 0.67 eV, and the corresponding radical density of the Ar-4p state is in the order of 10^{10}~10^{11} cm^{-3}. The variation of the excitation temperature is almost linear in relation to the operation voltage and the position of the plasma plume, meaning that the variation rates of the electron-excitation temperature are 0.03 eV/kV for the voltage and 0.075 eV/cm along the plasma plume.

Keywords: Plasmas, Plasma devices, Discharge, Atmospheric Pressure Discharge, spectroscopy.

I. Introduction

Ar spectroscopy has been studied fairly comprehensively [1,2], with most of the research concerning a low pressure and a high electron-energy; moreover, numerous papers regarding the spectroscopy of ambient-pressure Ar jets were reported over the last decade [3-14]. In the low-frequency operation of several tens kHz for an atmospheric-pressure Ar-plasma jet that was introduced recently [15], a low current and a low voltage are imperative for the protection of a human body from an electric shock and thermal damage; therefore, the operation range of the applied voltage is quite narrow. This study is concerned with the information regarding the radical species in the plasmas of such weak currents. The purpose of this study is the use of a spectroscopic investigation of Ar-jet plasma for the provision of radical-species information, including density, and the determination of the electron-excitation temperature. Specifically, variations of the excitation temperature and the excited-radical density according to the operation voltage and the plasma position are studied and discussed. The theory of the excitation temperature is described in Section 2. The experimental setup and the optical spectra are recorded according to the voltage variations and the measuring points in Section 3. With the use of the spectral data, the electron-excitation temperature and the radical density of the excited-Ar atoms are analyzed in Section 4. And the conclusion is presented in Section 5.

*Corresponding author
E-mail: gscho@kw.ac.kr

II. Excited Electron Temperature with a Relative Spectra-Intensity

Non-equilibrium plasma of an atmospheric pressure plasma jets (APPJs) is not relevant to the approximation of a local thermal equilibrium (LTE). LTE is applicable to the plasma of relatively high electron energy, for instant, a low pressure discharge-plasma [16-19]. In Boltzmann plots based on LTE, an electron excited temperature (T_{ex}) can be determined with the spectral transition-data in a quite wide range of energy level. Besides a low pressure discharge, LTE can be retained in the plasma of a high pressure discharge such as a microwave discharge [20-21] and an arc-discharge [22]. However, in APPJs operating with a low frequency of several tens kHz, it is hard to determine T_{ex} with the Boltzmann-plots because a high level transition would not appear in a general operation-voltage.

In this study of APPJs, we expand the operation range to a high voltage for a high energy-level transition with which we can estimate T_{ex} from the Boltzmann plots. Using the 'line-pair method [20]' comparing a spectrum intensity of a low voltage operation to the intensity of a high voltage operation, we interpolate T_{ex} for a low voltage operation

with the known value T_{ex} obtained for a high voltage operation. Even though the LTE approximation and the Boltzmann distribution are not proper in the analysis of APPJs, we expect to be able to have a ball-park figure in respect of T_{ex} and the related radical density.

An excitation temperature can be deduced from the absolute intensity of the atomic line by assuming a local thermal equilibrium. The formal excitation temperature corresponds to the electron energy that can excite atoms from the ground state to the excited state, and it is evaluated using the Boltzmann distribution; here, the relation between the population density of the atoms N_j that are in a state with energy E_j and the total number of atoms N_o in the system is determined [16-17], as $N_j = (N_o g_j/Z)\exp(-E_j/T_{ex})$ where T_{ex} is the electron-excitation temperature, g_j is the degeneracy of level-j, and Z is the partition function. When the atoms are in the excited state-j, which is decayed spontaneously to a level-i by radiative emission, the plasma emissivity I_{ji} is proportional to the number of atoms in the state-j according to the following equation:

$$I_{ji} = (f_c hc N_o/Z)A_{ji}(g_j/\lambda_{ji})\exp(-E_j/T_{ex}) \quad (1)$$

where h is Planck's constant, c is the velocity of light in a vacuum, A_{ji} is the Einstein coefficient, λ_{ji} is the wavelength of the emission, and f_c is the correction function related to the detection-sensitivity calibrations regarding factors such as the exposure time and the filtering.

The conventional Boltzmann-plot technique for the determination of the excitation temperature is represented by the formula of $\ln(I_{ji}\lambda_{ji}/A_{ji}g_j) = -(E_j/T_{ex}) + \text{constant}$. From the best fitting, the inverse of the slope gives the electron-excitation temperature T_{ex}. A Boltzmann plot is one of the most effective approaches for the determination of the T_{ex}; however, a greater accuracy is obtained if the used emission lines cover a wide excitation-energy range.

If the temperature T_{ex} is a known value, we have the excited density N_j where only the electron excitation collision is considered. The partition function of $Z = \Sigma g_j \exp(-E_j/T_{ex})$ is the sum of the weighted Boltzmann functions of all of the energy levels. If the ground state of $j = 0$, $E_o = 0$, and $g_o = 1$ is dominant in the partition function, which is the case regarding $E_j >> T_{ex}$ and the excited density of $N << N_o$ for the state of $j \geq 1$, $Z \sim 1$ is approximated, and this is valid for the Ar spectra if the first excited state satisfies at least $E_1 >> T_{ex}$.

A special case of the Boltzmann plot, the so-called 'line pair method [20]' for which the relative-line intensity is used, has also been employed in the determination of T_{ex}. Similarly, when the excitation temperature T_{exo} is known for a specific operation condition, the variation of T_{ex} according to the variation of the operation condition is estimated. If the optical intensity I_{ko} changes to I_k for the same spectrum λ_k and the transition-energy level E_k, the temperature T_{ex} is calculated as $I_{ko}/I_k = \exp[-E_k(1/T_{exo} + 1/T_{ex})]$; therefore, the relation is represented by the following:

$$1/T_{ex} = 1/T_{exo} - (1/E_k)\ln(I_k/I_{ko}) \quad (2)$$

III. Experiments and Spectra-Intensity

The schematic of the experimental setup, which is similar to those used in our previous works [23-28], is shown in Fig. 1. The main body of the plasma-jet system comprises a syringe needle. The inner diameter of the syringe needle is 0.9 mm, while its outer diameter is 1.3 mm. The syringe needle is inserted into a quartz tube with an inner diameter of 1.5 mm. The working Ar-gas is injected through a Teflon tube controlled by a mass-flow meter. The open end of the outer quartz tube is wrapped with copper foil of a 3 mm width and acts as an external ground electrode. The needle electrode is connected to high-voltage sinusoidal power that supplies a maximum voltage of 10 kV of an rms (root mean square) value with a 20 kHz frequency. The Ar-gas flow rate is fixed with Q = 2 lpm to keep a laminar flow in a glass tube with an inner diameter of $r_D = 1.5$ mm, where the Reynolds number is $R_n = 1.78 \times 10^3 (Q/r_D) = 2373$ [28].

An optical fiber (mounted vertically onto the axis of the jet) coupled with an Ocean Optics HR4000CG-UV-NIR spectrometer is used to obtain the spectra from the discharge plasma. The optical fiber is located in a perpendicular position 5 mm from the surface line of the glass tube. The spectral resolution and spectral range of the optical emission spectrometer are 0.75 nm and 200 nm to 1100 nm, respectively. The spectrometer is calibrated with a certified tungsten lamp for the production of corrected relative intensities. The gate time of the optical-intensity integration is adjustable from 4 ms to 20 s. The maximum intensity of the light emission is monitored at 150,000 counts, with a sensitivity of 100 photons per count. The function of the dark-current correction is used throughout the entire measurement.

The optical-emission spectra are measured according to the operation voltages that are applied to the syringe

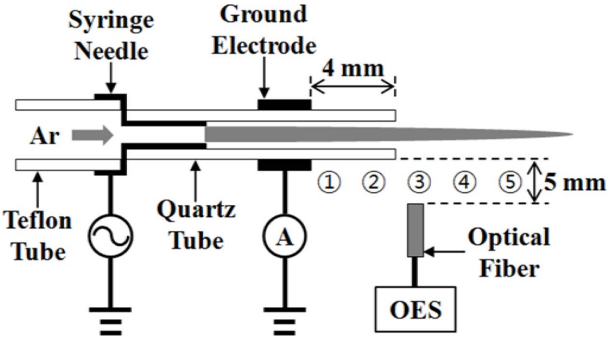

Figure 1. The schematic of the experimental setup for the OES measurement with the Ar-plasma jet comprising a syringe needle inserted into a glass tube.

electrode and the positions along the plasma column. The measuring points are located at distances of 1 mm, 3 mm, 5 mm, 7 mm, and 9 mm that are respectively noted with the numbers ①-⑤ from the end of the external ground electrode.

The spectra are obtained for operation voltages in the range from 2 kV to 5 kV, and the corresponding excited-plasma current is from 3 mA to 16 mA. Even if the operation voltage is recommended in the range of 2 kV to 3 kV, with a current from 3 mA to 7 mA for electrical safety (an electric shock is not experienced) regarding the human body, we measured the data in the range expanded from 2 kV to 8 kV for the analysis. At the voltage of 2 kV, the visual plasma reaches only the position ⑤ that is 9 mm from the end of the external electrode; moreover, for the increasing voltage of 3 kV to 5 kV, the plume length increases from approximately 10 mm to 25 mm.

The optical spectra are recorded according to the voltage variations and the measuring points in the subsections 3-1 and 3-2, respectively.

1. Spectra according to the voltage

At the fixed position ③ (the position of 5 mm) of the optical fiber, the plasma-emission spectra are measured with voltages of 2 kV, 3 kV, 4 kV, 5 kV, and 8 kV. The spectra are depicted in Fig. 2. With the operation voltages of 2 kV to 5 kV, only the red-line transitions of 4p→4s for the Ar spectra are appeared, whereby the blue-lines of the 5p→4s transitions are not observed. However, it is necessary to have a wide range of excitation-energy levels for the exact value of the electron-excitation temperature T_{ex} by fitting in the Boltzmann plot. For the Ar spectra of a high-energy-level transition from the 5p level, an additional experiment with the high voltage 8 kV is conducted and the new Ar spectra of 5p→4s are observed even if the corresponding optical intensity is low.

In the experiments for the 2 kV to 5 kV range, the exposure time is 500 ms; however, when we use the exposure time of 500 ms for the high voltage of 8 kV, the intensity in our OES exceeds the maximum limitation intensity of 150,000 (photon counts). We therefore reduced the exposure time to 40 ms, and the measured value of the optical intensity is instead adjusted by 12.5 times since the intensity has been verified to be exactly proportional to the exposure time. The intensity for 8 kV is therefore adjusted by a multiplication of 12.5 times for a comparison with the intensity data of 2 kV to 5 kV. The relative intensity according to the exposure time has been verified by the OES calibration.

The spectra are the same kind as those that appeared in the operation of the low voltages from 2 kV to 8 kV except the spectra of 5p→4s for 8 kV. The typical high-intensity lines of Ar-transitions 4p→4s in the emission spectra range of 700 nm to 900 nm, such as 763 nm, 811 nm, and 912 nm, appeared [9-10]. The line of 811 nm, the highest

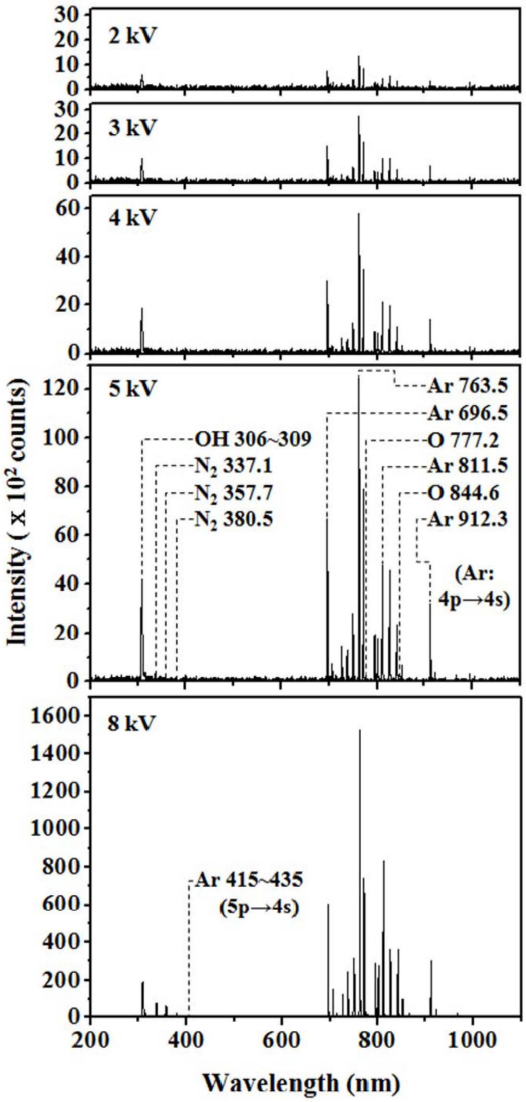

Figure 2. Optical-emission spectrum measured at ③ (5 mm from the end of the external electrode) with the applied voltages of 2 kV, 3 kV, 4 kV, 5 kV, and 8 kV on the Ar-plasma jet.

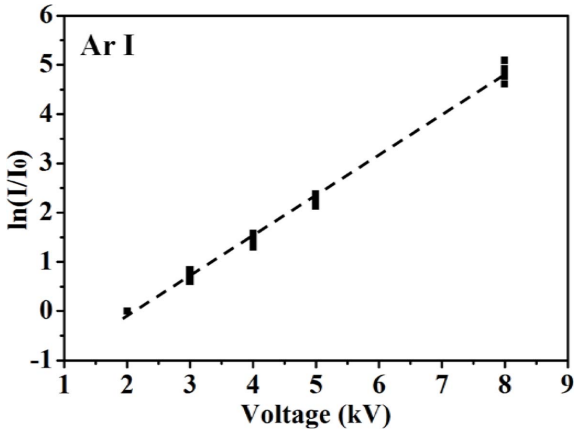

Figure 3. The variation of the optical-emission intensity according to the operation voltage is presented for the spectra of Ar. The log value of intensity I that is normalized by the intensity I_o of 2 kV is proportional to the voltage so that the intensity of all of the Ar spectra varies as $I = I_o\exp(+0.74\ V)$, as noted by the fitting line.

line of the low-pressure Ar discharge, is often used for the monitoring of the population of the argon meta-stable level by absorption [10]; however, as has often appeared in other studies, the highest line of the atmospheric-pressure Ar jet is 763 nm [10,29-30].

Figure 3 depicts the variation of the optical intensity according to operation voltages from 2 kV to 5 kV. The plot presents $\ln(I/I_o)$ versus voltage V, where the spectral intensity I is normalized by the reference intensity I_o of the lowest voltage of 2 kV. The intensity increases exponentially according to the increasing voltage with an increasing rate that is almost the same; in particular, the intensity increase of the Ar spectra shows exactly the same slope of approximately 0.74 when it behaves as a function of $I = I_o\exp(+0.74\ V)$. The intensities of all of the Ar spectra therefore vary with the electron-excitation temperature that is also changed linearly according to the operation voltage; this will be shown again in the following section 4, where the excitation temperature will be determined according to the variation of the optical intensity.

2. Spectra according to the position of the plasma column

For a fixed voltage of 3 kV, the spectra are shown in Fig. 4 with the several measuring points. The distances of 1 mm at ① and 3 mm at ② are in the glass-tube inside

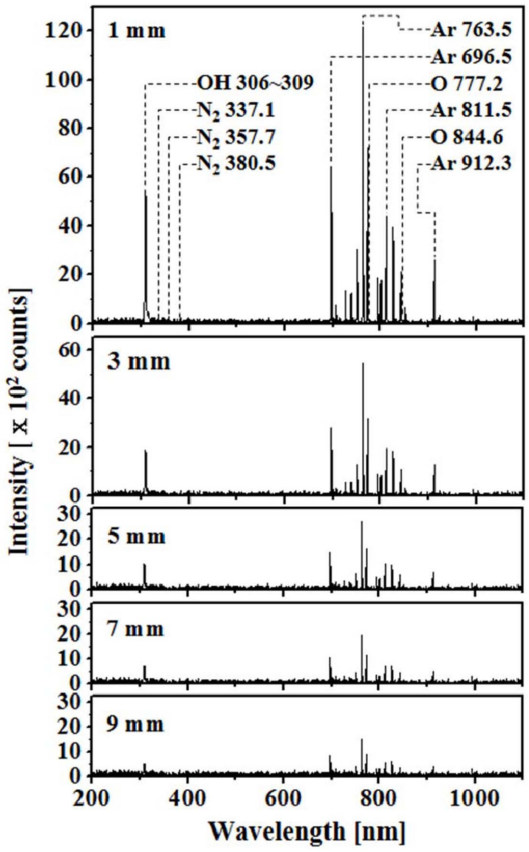

Figure 4. Optical-emission spectrum measured along the effluent plasma at the positions of ① to ⑤ noted in Fig. 1 with the applied voltage of 3 kV.

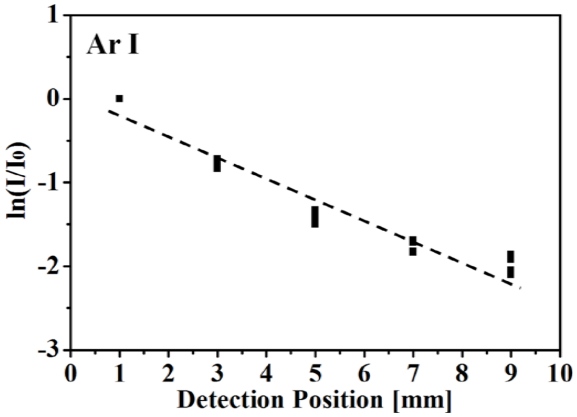

Figure 5. The variation of the optical-emission intensity according to the detection position is presented for the spectra of Ar. The log value of intensity I that is normalized by the intensity I_o of 1 mm is negatively proportional to the position x so that the intensity varies as $I = I_o\exp(-0.25x)$, as noted by the fitting line.

nozzle; the other three positions in the outside nozzle in the open air are 5 mm at ③, 7 mm at ④, and 9 mm at ⑤. The numbers of ①-⑤ are noted in Fig. 1. The distance in mm is from the end of the external ground electrode. The species of the spectra in Fig. 2 and Fig. 4 are the same kinds, but the optical intensity varies according to the voltage and the measuring position.

Figure 5 presents the variation of the optical intensity along the positions of the effluence plasma for the Ar-spectra. The reference intensity I_o is taken at the position of 1 mm for the relative intensity I at the other positions in the range of 2 mm to 9 mm. The graph is plotted between $\ln(I/I_o)$ and the position x = (1-9) mm. Similar to Fig. 2, the relative intensities of the Ar-spectra decay exponentially with a decay rate that is almost the same as the increasing distance x from the plasma, from the inside of the glass to the outside. The slope of the exponent decay rate is 0.25 in the graph; therefore, the optical intensity is interpolated as $I = I_o\exp(-0.25x)$. The electron-excitation temperature can be evaluated using the variation of the optical intensities of the Ar spectra in the following subsection 4.

IV. Analysis of Excitation Temperature

In the previous section 3 of our experiments, we observe the Ar-spectra of 4p→4s for 2~5 kV and 8 kV and the 5p →4s Ar-spectra only for 8 kV. As it has been mentioned in section-2, Ar-spectra intensity data are applied to the Boltzmann plots and the line-pair method.

We observe only the red-line transition of 4p→4s for the Ar spectra with the operation voltages of 2 kV to 5 kV, whereby the blue-lines of the 5p→4s transitions are not observed; therefore, we do not have a wide range of excitation-energy levels, making it difficult to obtain the exact value of the electron-excitation temperature T_{ex} by fitting in the Boltzmann plot. In Fig. 6(a), the data points

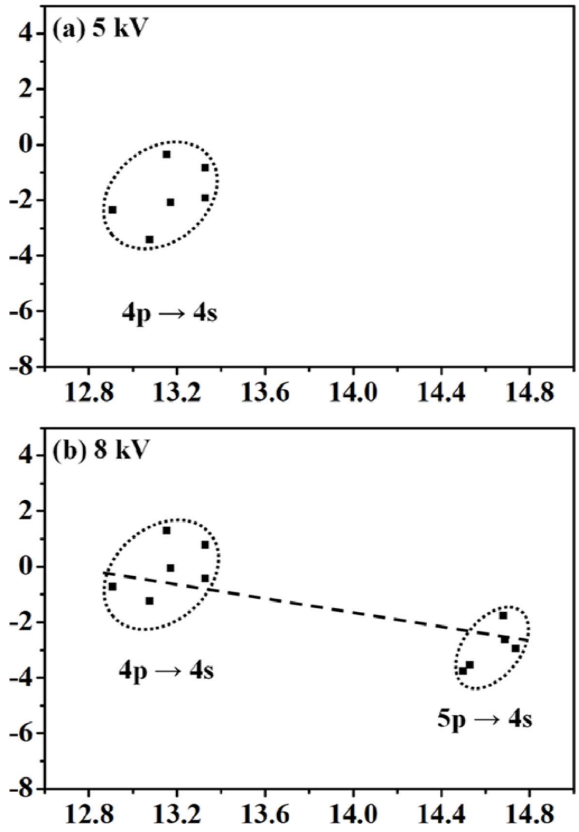

Figure 6. Boltzmann plot with Ar spectra measured at 5 mm with 5 kV in (a) where the line fitting is not available. Boltzmann plot with the data listed in Table 3 with 8 kV in (b) where the excitation temperature of T_{ex} = 0.79 eV is estimated from the inverse value of the slope of 1.27 with the fitting line.

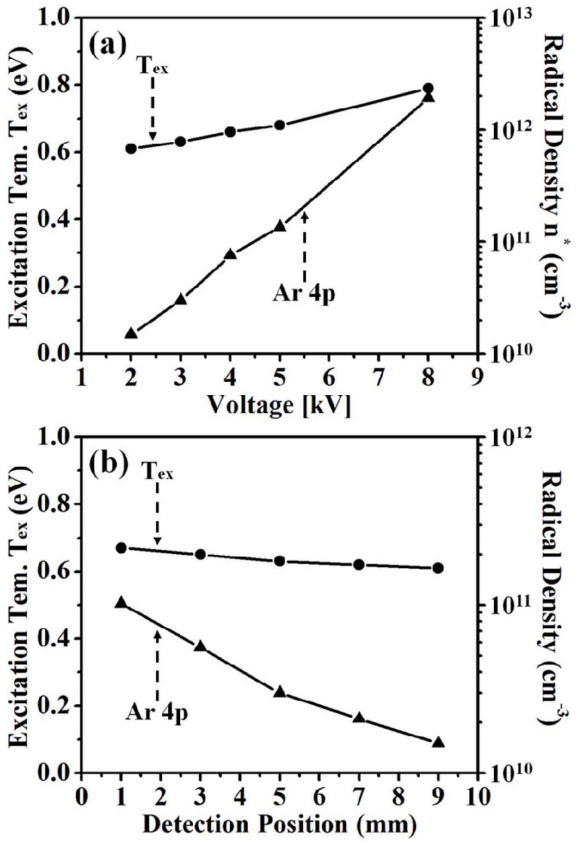

Figure 7. (a) For the operation voltage of V = (2-5) kV and 0.79 eV for 8 kV, the electron-excitation temperature (left axis) is plotted as T_{ex} = (0.61-0.68) eV. The increasing rate of T_{ex} over the voltage is 0.03 eV/kV approximately. The corresponding radical densities (right axis) of the Ar-4p are N_{4p} = (1.5-13.5) × 10^{10} cm^{-3} for V = (2-5) kV. (b) For the detection position of (1-9) mm, the excitation temperature is drawn as T_{ex} = (0.67-0.61) eV. The variation rate of the temperature is 0.075 eV/cm. The corresponding radical density of the Ar-4p state is N_{4p} = (10.2-1.5) × 10^{10} cm^{-3} with the operation voltage of 3 kV.

of the Boltzmann plots are depicted for the operation voltage of 5 kV and the measuring position of 5 mm for the Ar spectra in Fig. 2. Notably, the attainment of a slope by fitting the data point in a narrow energy range like that of Fig. 6(a) is impossible.

For the purpose of obtaining the Ar spectra of a high-energy-level transition from the 5p level, an additional experiment with a high operation voltage needs to be conducted. In the Ar-spectra for the voltage of 8 kV and the position of 5 mm, the new Ar spectra of 5p⟶4s are observed even if the corresponding optical intensity is low. The other spectra are the same kind as those that appeared in the operation of the low voltages from 2 kV to 5 kV.

Figure 6(b) presents the Boltzmann plot with the data of the 4p-transition spectra and the 5p-transition spectra for the operation voltage of 8 kV. The slope of 1.27 is obtained by fitting the data points, and the electron-excitation temperature is T_{ex} = 0.79 eV from the inverse value of the slope.

By using Eq. (2) with the reference values of the excitation temperature T_o = 0.79 eV and the optical intensity I_o for 8 kV, the temperature T for 2 kV to 5 kV is interpolated by comparing the Ar intensity I; the results are presented in Fig. 7(a). For the operation voltage of V = (2, 3, 4, 5) kV, the average temperature value regarding all of the Ar spectra is evaluated as $T_{ex} \pm \Delta T$ = (0.61, 0.63, 0.66, 0.68) ± 0.003 eV. The deviation value of ΔT is not high since, remarkably, the intensity variation of all of the Ar spectra is proportional to the voltage variation, as shown in Fig. 3. The increasing rate of the excitation temperature according to the voltage is 0.03 eV/kV, which is the slope in Fig. 7(a).

From the use of Eq. (1) with Z~1 and $N_o \approx 2.7 \times 10^{19}$ cm^{-3} (Loschmidt's number), the density of an excited Ar state is obtained. For the voltage variation V = (2, 3, 4, 5, 8) kV, the density of the excited-Ar state of the 4p level (~13 eV) is n*(Ar-4p) = (1.5, 3.0, 7.6, 13.5, 191.0) × 10^{10} cm^{-3}. In the voltage range of 2 kV to 5 kV, the density of the excited-Ar radial varies in the order from 10^{10} cm^{-3} to 10^{11} cm^{-3}; if the voltage increases to 8 kV, the density increases to 10^{12} cm^{-3}. These orders of the Ar-radical density are in sound agreement with the results reported in Ref. [10]. Figure 7(b) presents the electron-excitation temperature and the excited-Ar-radical density that are estimated with the variation of the optical intensity

for the Ar spectra, which are measured along the position of the effluent plasma. Using Eq. (2) with the reference temperature T_o = 0.63 eV and the intensity I_o for 3 kV and 5 mm obtained in Fig. 7(a), the average temperature for all of the Ar spectra is calculated as $T_{ex} \pm \Delta T$ = (0.67, 0.65, 0.63, 0.62, 0.61) ± 0.003 eV and corresponds to the positions of (1, 3, 5, 7, 9) mm. The variation rate of the temperature per cm is 0.075 eV/cm.

The Ar-radical density is also evaluated in Eq. (1). For the state of the 4p level (~13 eV), the excited-Ar density is n*(Ar-4p) = (10.2, 5.6, 3.0, 2.1, 1.5) × 10^{10} cm^{-3} and corresponds to the positions of (1, 3, 5, 7, 9) mm. The density of the excited-Ar-4p level decreases from 10^{11} cm^{-3} inside the glass tube to 10^{10} cm^{-3} outside the nozzle.

The electron-excitation temperature has been reported for an Ar-plasma jet with the same kind of syringe electrode, but with the different operation scheme of a double electrode [29]; here, the authors measured the Ar spectra at a distance of approximately 5 cm from the tip of the syringe electrode, and the excitation temperature from the Boltzmann plot is reported as approximately T_{ex}~0.25 eV. If the temperature reduction rate of 0.075 eV/cm that was obtained in our experiment is considered along the position of the plasma, the temperature is T_{ex}~0.625 eV, with a temperature reduction of 0.375 eV for a distance of 5 cm from the position of the plasma generation; in this case, the magnitude of the excitation-temperature result [29] is the same as that of this paper. A paper also reported an excitation temperature of T_{ex}~0.45 eV for the Ar jet in a pulsed DC of 2.4 kV, with 20 kHz and duty cycles of 10%; here, the excitation temperature depends on the average power [29].

IV. Conclusions

The optical-emission spectra are analyzed in a pencil-type Ar jet comprising a syringe needle inserted into a glass tube. For biomedical applications where the plasma is generated by a sinusoidal voltage of a 20 kHz frequency, it is necessary to maintain a low-voltage operation (a few kV) to ensure safety regarding electricity.

The same types of spectra are observed independently on the operation voltages and the measuring positions, while only the optical intensity varies accordingly. Ar spectra of 4p→4s transition are observed as the red line of 696 nm to 965 nm, while the Ar spectra of 5p→4s will not appear at a low voltage. A wide range of transition energy is necessary in a Boltzmann plot for the determination of the electron-excitation temperature by the fitting of the spectral data; in the Ar spectra, a red line of the 4p level (12.9 eV to 13.5 eV) and a blue line of the 5p level (14.4 eV to 14.8 eV) are both required. Since the intensity of the 5p-transition spectra is always low, the blue line will not be measured for a low-voltage operation; therefore, the spectral data of the 5p transition for a high-voltage operation is needed to determine the excitation temperature from the Boltzmann plot. By using the reference temperature and the intensity obtained from a high-voltage operation, an excitation temperature of a low voltage is interpolated with the relative optical intensity.

For the 8 mm measuring distance of the plasma-jet plume, the electron-excitation temperature has been estimated as T_{ex} = (0.67-0.61) eV, while the corresponding excited-Ar density of the 4p state is in a low-voltage range of (1.0210^{11} -1.5 × 10^{10}) cm^{-3}. The temperature is high at the side of the plasma generation, and it reduces as the position moves further from the active region of the cavity. For the variation of the voltage in the range of 2 kV to 8 kV, the T_{ex} is (0.61-0.79) eV and the Ar-radical density varies from 10^{10} cm^{-3} to 10^{12} cm^{-3}. The variation rates of the electron-excitation temperature and the plasma plume of the Ar jet are 0.075 eV/cm and 0.03 eV/kV, respectively.

Similar to the variations of the voltage and the position, the variation of the optical intensities of the Ar spectra is exponential. Since the rate of the intensity variation is exactly the same for all of the Ar spectra, it is possible to estimate the approximate data of the electron-excitation temperature and the Ar-excitation density in this study.

Acknowledgements

This work was supported by the Korea Institute of Energy Technology Evaluation and Planning (KETEP) and the Ministry of Trade, Industry & Energy (MOTIE) of the Republic of Korea (20173030014460).

References

[1] W. Wiese, J. Brault, K. Danzmann, V. Helbig, and M. Kock, Phys. Rev,. A 39, 2461 (1989).
[2] A. Bogaerts, R. Gijbels, and J. Vlcek, Spectrochimica Acta Part B: Atomic Spectroscopy, 53, 1517 (1998).
[3] A. Sarani, A. Nikiforov, and C. Leys, Phys.Plasmas, 17, 063504 (2010).
[4] S. Förster, C. Mohr, and W. Viöl, Surface Coat. Technol., 200 (2005) 827.
[5] A. Nikiforov, A. Sarani, and C. Leys, Plasma Sour. Sci. Technol., 20, 015014 (2011).
[6] S. Yugeswaran and V. Selvarajan, Vacuum, 81, 347 (2006).
[7] T. Ichiki, T. Koidesawa, and Y. Horiike, Plasma Sour. Sci. Technol., 12, S16 (2003).
[8] S. Reuter, J. Winter, A. Schmidt-Bleker, D. Schroeder, H. Lange, N. Knake, V. Gathen, and K. Weltmann, Plasma Sour. Sci. Technol., 21, 024005 (2012).
[9] X. Guimin, Z. Guanjun, S. Xingmin, M. Yue, W. Ning, and L. Yuan, Plasma Sci. Technol., 11, 83 (2009).
[10] Q. Xiong, A. Nikiforov, N. Britun, R. Snyders, C. Leys, and X. Lu, J. Appl. Phys., 110, 73302 (2011).
[11] D. Staack, B. Farouk, A. Gutsol, and A. Fridman, Plasma Sour. Sci. Technol., 17, 025013 (2008).
[12] D. Mariotti, Y. Shimizu, T. Sasaki, and N. Koshizaki, J. Appl. Phys., 101, 013307 (2007).
[13] A. Rahman, A. Yalin, V. Surla, O. Stan, K. Hoshimiya, Z. Yu, E. Littlefiled, and G. Collins, Plasma Sour. Sci. Technol., 13, 537 (2004).
[14] X. Zhu, W. Chen, and Y. Pu, J. Phys. D: Appl. Phys., 41, 105212 (2008).

[15] Y. Kim, S. Jin, G. Han, G. Kwon, J. Choi, E. Choi, H. Uhm, and G. Cho, IEEE Trans. Plasma Sci., 43, 944 (2015).
[16] A. Chingsungnoen, J. Wilson, V. Amornkitbamrung, C. Thomas, and T. Burinprakhon, Plasma Sour. Sci. Technol., 16, 434 (2007).
[17] T. Chung, H. Kang, and M. Bae, Phys. Plasmas, 19, 113502 (2012).
[18] F. J. Gordillo-Vázquez, M. Camero, and C. Gómez-Aleixandre, Plasma Sources Science and Technology, 15, 42 (2005).
[19] S. Darwiche, M. Nikravech, S. Awamat, D. Morvan, and J. Amouroux, Journal of Physics D: Applied Physics, 40, 1030 (2007).
[20] Q. Jin, Y. Duan, and J. Olivares, Spectrochimica Acta Part B: Atomic Spectroscopy, 52, 131 (1997).
[21] A. Sola, M. D. Calzada, and A. Gamero, Journal of Physics D: Applied Physics, 28, 1099 (1995).
[22] J. Mirapeix, A. Cobo, O. M. Conde, C. Jaúregui, and J. M. López-Higuera, NDT & E International, 39, 356 (2006).
[23] G. Cho, H. Lim, J. H. Kim, D. J. Jin, G. C. Kwon, E. H. Choi, and H. S. Uhm, IEEE Trans. Plasma Sci., 39, 1234 (2011).
[24] G. Cho, J. Kim, H. Kang, Y. Kim, G. Kwon, and H. Uhm, J. Appl. Phys., 112, 103305 (2012).
[25] G. Cho, H. Kang, E. Choi, and H. Uhm, IEEE Trans. Plasma Sci., 41, 498 (2013).
[26] J. Jeong, Y. Kim, M. Lee, G. Han, H. Kim, D. Jin, J. Kim, E. Choi, H. Uhm, and G. Cho, J. Kor. Phys. Soc., 61, 557 (2012).
[27] K. Baik, H. Kang, J. Kim, S. Park, J. Bang, H. Uhm, E. Choi, and G. Cho, Appl. Phys. Lett., 103, 164101 (2013).
[28] D. Jin, H. Uhm, and G. Cho, Phys. Plasmas, 20, 083513 (2013).
[29] M. Qian, C. Ren, D. Wang, J. Zhang, and G. Wei, J. Appl. Phys., 107, 063303 (2010).
[30] L. Taghizadeh, A. Nikiforov, R. Morent, J. Mullen, and C. Leys, Plasma Process. Polym., 11, 777 (2014).
[31] Z. Machala, M. Janda, K. Hensel, I. Jedlovský, L. Leštinská, V. Foltin, V. Martišovitš, and M. Morvova, J. Molecul. Spectros., 243, 194 (2007).
[32] W. Wiese, M. Smith, and B. Glennon, *Atomic Transition Probabilities Volume I Hydrogen Through Neon* (US Government Printing Office, Washington, DC, 1966), pp. 1-153.
[33] W. Wiese, M. Smith, and B. Miles, *Atomic Transition Probabilities Volume II Sodium through calcium* (US Government Printing Office, Washington, DC, 1969), pp. 1-269.
[34] R. Pearse and A. Gaydon, *The Identification of Molecular Spectra* (Chapman and Hall, London, 1950), pp.1-276.
[35] G. Bastiaans and R. Mangold, Spectrochimica Acta Part B: Atomic Spectroscopy, 40, 885 (1985).
[36] G. Norlén, Physica Scripta, 8, 249 (1973).